Clin Orthop Relat Res (2008) 466:782–790
DOI 10.1007/s11999-008-0141-7

SYMPOSIUM: DEVELOPMENTAL DYSPLASIA OF THE HIP

Femoral Morphology Differs Between Deficient and Excessive Acetabular Coverage

**S. D. Steppacher MD, M. Tannast MD,
S. Werlen MD, K. A. Siebenrock MD**

Published online: 21 February 2008

Abstract Structural deformities of the femoral head occurring during skeletal development (eg, Legg-Calvé-Perthes disease) are associated with individual shapes of the acetabulum but it is unclear whether differences in acetabular shape are associated with differences in proximal femoral shape. We questioned whether the amount of acetabular coverage influences femoral morphology. We retrospectively compared the proximal femoral anatomy of 50 selected patients (50 hips) with developmental dysplasia of the hip (lateral center-edge angle [LCE] $\leq 25°$; acetabular index $\geq 14°$) with 45 selected patients (50 hips) with a deep acetabulum (LCE $\geq 39°$). Using MRI arthrography we measured head sphericity, epiphyseal shape, epiphyseal extension, and femoral head-neck offset. A deep acetabulum was associated with a more spherical head shape, increased epiphyseal height with a pronounced extension of the epiphysis towards the femoral neck, and an increased offset. In contrast, dysplastic hips showed an elliptical femoral head, decreased epiphyseal height with a less pronounced extension of the epiphysis, and decreased head-neck offset. Hips with different acetabular coverage are associated with different proximal femoral anatomy. A nonspherical head in dysplastic hips could lead to joint incongruity after an acetabular reorientation procedure.
Level of Evidence: Level IV, retrospective comparative study. See the Guidelines for Authors for a complete description of levels of evidence.

One or more of the authors (SDS, MT, KAS) has received funding from the National Center for Competence in Research "Computer Aided and Image Guided Medical Interventions (Co-Me)" of the Swiss National Science Foundation (SNF).
Each author certifies that his or her institution has approved the human protocol for this investigation and that all investigations were conducted in conformity with ethical principles of research.

S. D. Steppacher, M. Tannast (✉), K. A. Siebenrock
Department of Orthopaedic Surgery, Inselspital, University of Bern, Murtenstrasse, 3010 Bern, Switzerland
e-mail: moritz.tannast@insel.ch

S. Werlen
Department of Radiology, Sonnenhof Clinic, Bern, Switzerland

Introduction

Acetabular and femoral abnormalities are often combined because the final acetabular shape and depth depends on the interaction with a spherical femoral head [16]. For example, hips with Legg-Calvé-Perthes disease or proximal femoral focal deficiency have a higher incidence of dysplasia, acetabular retroversion, and incongruity [4–6]. This might be due to a premature or eccentric fusion of the triradiate cartilage with subsequent alterations of the articular cartilage and changes of the acetabular dimension [12]. Kitadai et al. [14] suggested the lateral center-edge (LCE) angle was increased in patients with slipped capital femoral epiphysis compared to those with normal hips. These observations have been supported by rat models in which the femoral heads were dislocated or excised [9] and subsequent acetabular remodeling was seen in hips where a femoral osteotomy was performed for better joint containment [18].

Many studies [4–6, 9, 12, 14, 16, 18] suggest a primary abnormality of the femoral head may subsequently affect the acetabular shape secondarily. Based on the observations in more than 1000 surgical hip dislocations for treatment of excessive acetabular coverage and 700

periacetabular osteotomies for treatment of developmental dysplasia of the hip (DDH) at the senior author's (KAS) institution, we observed the femoral head shape substantially differs in relation to acetabular coverage.

We therefore questioned if dysplastic hips have (1) a more aspherical femoral head; (2) a decreased epiphyseal height; (3) a less-pronounced extension of the epiphysis towards the femoral neck; and (4) a decreased femoral head neck offset compared to hips with a deep acetabulum. Additionally, we presumed the femoral head sphericity depends on the epiphyseal height.

Materials and Methods

Using our digital institutional database, we retrospectively identified 421 patients (480 hips) with documented symptomatic DDH or a deep acetabulum (pincer-type

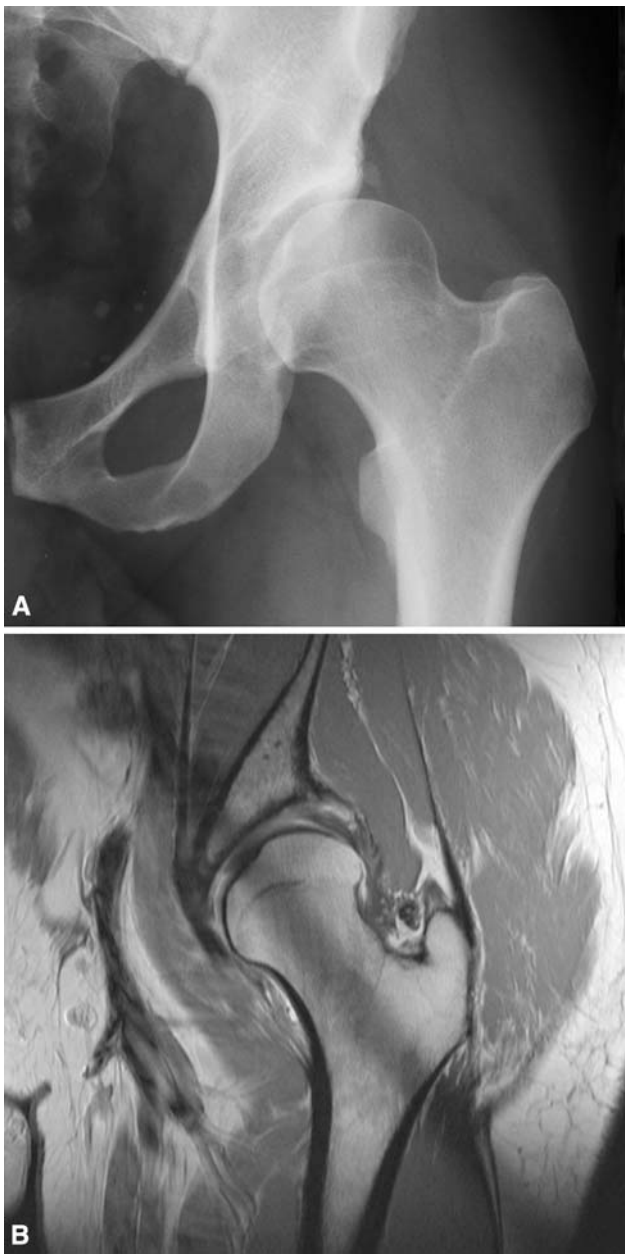

Fig. 1A–B A left hip from a 48-year-old male patient in the dysplastic group (Group I). (**A**) On the conventional AP pelvic radiograph the AI is 30° and the LCE is 3°. (**B**) On the corresponding coronal slice of the arthro-MRI decreased coverage is apparent, as is a compensatory thickened labrum.

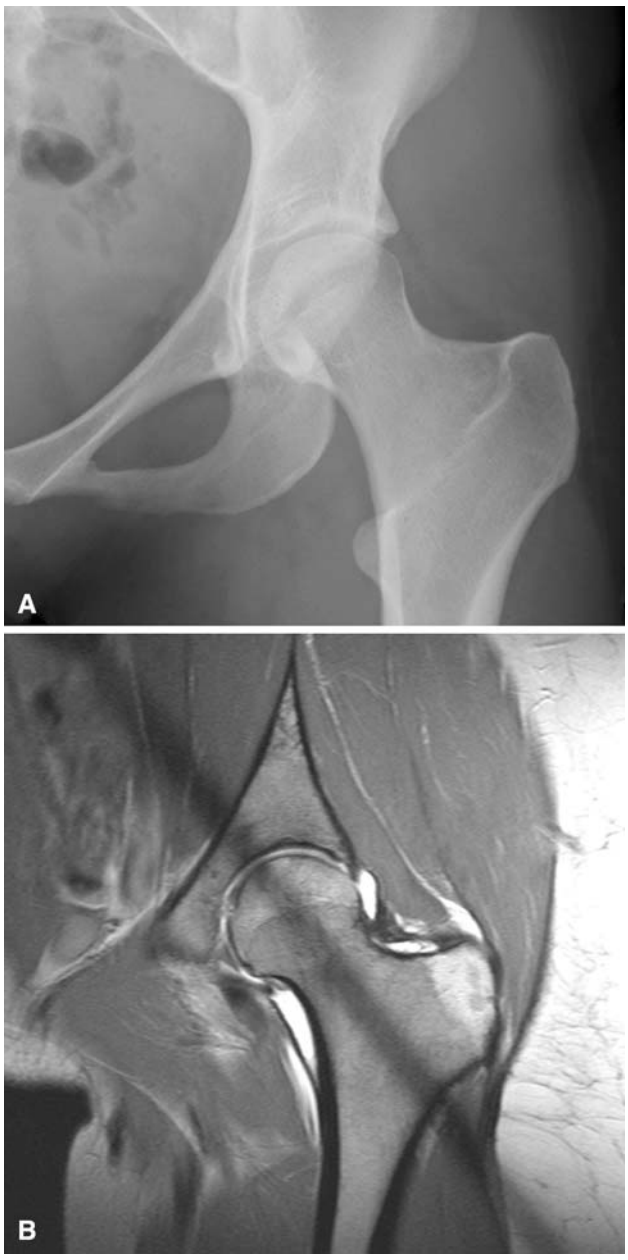

Fig. 2A–B A left hip from a 23-year-old female patient in the deep acetabulum group (Group II). On the (**A**) conventional AP pelvic radiograph the AI is 4° and the LCE is 42°. (**B**) On the corresponding coronal slice of the arthro-MRI the femoral head has excessive acetabular coverage.

Table 1. Comparison of demographic and radiographic data of the dysplasia (Group I) and the deep acetabulum (Group II) groups

Parameter	Dysplasia group (Group I)	Deep acetabulum group (Group II)	p Value
Hips (n)	50	50	—
Age (years)*	33 ± 9.4 (17–49)	32 ± 10.3 (17–50)	0.496
Gender (% male)	26	36	0.387
Right hips (%)	48	48	1.000
Bilateral cases (%)	0	11	0.021
Weight (kg)*	70 ± 15 (48–110)	68 ± 14 (37–105)	0.428
Height (cm)*	170 ± 9 (151–188)	170 ± 9 (155–192)	0.884
Crowe classification [3] (Number of hips [%])			
Class I	50 (100%)	0	
Class II	0	0	
Class III	0	0	
Class IV	0	0	
Lateral center-edge angle [41] (degrees)*	14 ± 9 (−16–24)	44 ± 5 (39–59)	< 0.001
Acetabular index [39] (degrees)*	21 ± 6 (14–38)	−1 ± 5 (−13–14)	< 0.001
Extrusion index [22] (%)*	34 ± 7 (22–57)	9 ± 4 (0–16)	< 0.001
Craniocaudal femoral coverage (%)*	63 ± 12 (32–87)	92 ± 6 (79–100)	< 0.001
Neck shaft angle (degrees)*	137 ± 7 (123–151)	129 ± 7 (112–143)	< 0.001

* Mean ± standard deviation (range).

femoroacetabular impingement [7]) seen at the outpatient clinic between November 1997 and October 2006 with an age less than 50 years. A specific MRI arthrography for the hip had been performed in these cases [17]. We excluded 42 patients with a history of known hip disorders (including Legg-Calvé-Perthes disease, avascular necrosis of the femoral head, slipped capital femoral epiphysis, proximal femoral focal deficiency, Morbus Paget, tumor of the proximal femur) and 79 patients with previous hip surgery. Additionally, patients with skeletally immature hips (Stage ≤ 4 according to Risser [27]) ($n = 6$), advanced osteoarthritis (Grade ≥ 2 according to Tönnis [38]) ($n = 12$), incomplete or insufficient radiographic documentation ($n = 4$), or unidentifiable epiphyseal scar on the MRI slices were excluded ($n = 36$). These exclusions left 242 patients. We then compared the anatomy of the proximal femur between two groups with different amounts of acetabular coverage: one with deficient (dysplasia, Group I) (Fig. 1A-B) and one with excessive acetabular coverage (deep acetabulum, Group II) (Fig. 2A-B).

Dysplasia of the hip (Group I) was defined as an LCE angle of less than 25° [22] with a minimal acetabular index (AI) of 14° [39] and was classified according to Crowe et al. [3]. Hips with a deep acetabulum (Group II) were defined as hips with a LCE angle exceeding 39° on anteroposterior (AP) pelvic radiograph [39]. These radiographic criteria were not satisfied by 147 patients leaving 95 patients (100 hips, five bilateral) for evaluation; 50 patients (50 hips) for Group I and 45 patients (50 hips) for Group II. The two groups were comparable demographically except for the greater number of patients with bilateral DDH in Group II (Table 1). Because these numbers represented the maximum available numbers that fulfilled the inclusion criteria, we performed no a priori power analysis. Rather, we performed a post hoc power analysis for the primary research question (sphericity index) with a two-sided level of significance of 5% and found a power of 100%. This study was approved by the local institutional review board.

We obtained AP pelvic radiographs in a standardized manner to reduce the influence of individual pelvic tilt and rotation on measured radiographic parameters [36]. The patient was in supine position with internally rotated legs (approximately 20°) to compensate for femoral antetorsion. The film-focus distance was 1.2 m. The central beam was directed to the midpoint between the symphysis and a line connecting the anterosuperior iliac spines [35].

To further describe the morphology of the two study groups the extrusion index [22], the neck shaft angle [38], and the quantification of femoral head coverage were assessed by one observer (SDS) with the help of a previously developed and validated computer software called Hip^{2}Norm (University of Bern, Switzerland) (Table 1) [34, 37, 43].

The MRI arthrography was obtained according to the standardized technique described earlier [17]. Briefly, the scans were carried out on a Siemens Vision 1.5-T high-field scanner (Erlangen, Germany) using a flexible surface coil after fluoroscopic-guided intraarticular injection of saline-diluted gadolinium-DTPA (Dotarem 1:200, Guerbert

AG, Paris). The patients were positioned supine (analogously to the conventional radiography), and the lower extremities were fixed with 20° internal rotation of the hip to prevent motion during scanning and to generate standard version of the femoral neck and a standardized position of the pelvis. After obtaining transversal, sagittal, and coronal proton-density-weighted (PDW) and T1-weighted sequences to assess the entire joint, a radial PDW sequence was used in which all slices were oriented orthogonal to the femoral neck and head. These slices were based on a sagittal oblique localizer, which was marked on the PDW coronal sequence, running parallel to the sagittal oblique course of the femoral neck. For every patient these slices were defined individually resulting in 14 radial slices. Of these 14 slices every second slice was chosen, providing seven radial slices with 14 positions for measuring (Fig. 3A-B). Slice 1 was defined as the coronal slice and the subsequent slices were acquired rotating clockwise around the neck axis in 25.7° steps.

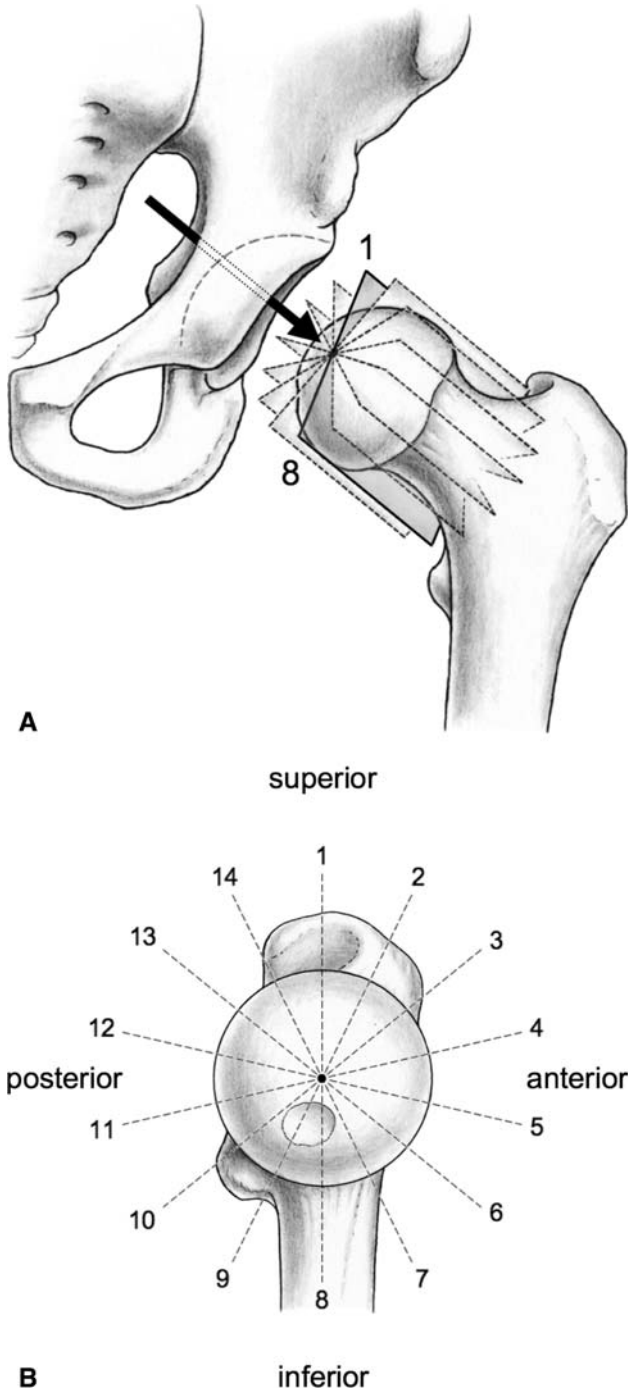

Fig. 3A–B (**A**) MRI arthrography of the left hip with seven slices perpendicular to the neck axis was chosen for accurate and comparable measurements of the femoral head morphology and the epiphyseal extent. The arrow indicates the view direction for the scout view. (**B**) Each slice on the scout view is obtained by rotating clockwise in 25.7° steps around the neck axis. These slices provide 14 positions for measuring the alpha and epiphyseal angles.

We measured four parameters: head sphericity (Fig. 4A), epiphyseal index (Fig. 4B), epiphyseal angle (Fig. 4C), and alpha angle (Fig. 4C) (Table 2). The head sphericity and the epiphyseal index were measured once per slice resulting in seven measurements per parameter and hip joint. In contrast, the epiphyseal angle and the alpha angle were measured at both articular surfaces of the femoral head-neck and therefore twice per slice or 14 times per joint. If a nonspherical shape of the femoral head was identified, the orientation of the elliptic head was measured with the angle between the neck axis and the major axis of the best-fitting ellipse. To adjust for different head sizes, only ratios and angles were calculated. All parameters were analyzed with commercially available software Osirix (Version 2.6, Geneva, Switzerland) [29].

In order to detect the reproducibility and reliability of these measurements, 35 MRI slices were randomly chosen from the image database. The blinded images were analyzed by two independent observers (SDS, MT) on two separate occasions at least one month apart. Intra- and interobserver variations in measuring the femoral head parameters were assessed using the intraclass correlation coefficient (ICC) (Table 3).

We confirmed normal distributions for all data with the Kolmogorov-Smirnov test. Unpaired Student's t-test was used for comparison of the two groups. To assess associations between categorical variables, the Fisher's exact test was performed. Correlation between the femoral head sphericity (dependent variable) and the epiphyseal height (independent variable) was verified with the Pearson's correlation test.

Results

We observed a more oval ($p < 0.001$) configuration of the femoral head in Group I (mean head sphericity index,

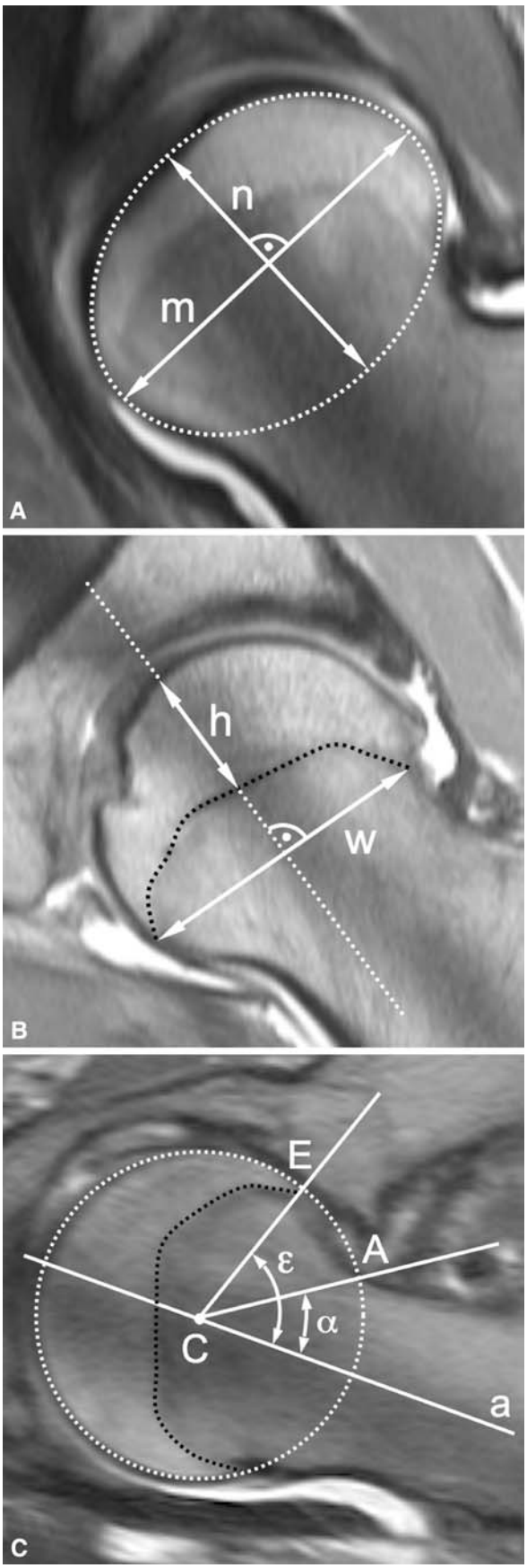

◀ **Fig. 4A–C** These radial arthro-MRI slices show the construction of the measured parameters. (**A**) The head sphericity is the ratio of the minor axis (n) to the major axis (m) of the ellipse. (**B**) The epiphyseal index is the ratio of the epiphyseal height (h) to epiphyseal weight (w). (**C**) The alpha angle (α) is formed by the neck axis (a) and a line through the center of the head [C] and the offset-point [A]. The epiphyseal angle (ε) is formed in a similar way with a line through the center of the head [C] and the point [E] where the epiphysis meets the articular surface.

0.83 ± 0.07; range, 0.80–0.87) compared to the more round configuration of Group II (mean, 0.99 ± 0.06; range, 0.97–1) (Table 4). The angle to describe the orientation of the elliptic femoral heads in Group I was 90° ± 7.5° (range, 89°–92°).

The epiphyseal index was reduced ($p < 0.001$) for Group I (mean index, 0.33 ± 0.05; range, 0.32–0.35) compared to Group II (mean, 0.42 ± 0.05; range, 0.41–0.43) (Table 4).

The mean epiphyseal angle was increased ($p = 0.001$–0.006) in all slices except slices 8, 9, and 13 for Group I (Table 5). For both groups, the maximum epiphyseal angle was located on slices 7 to 9 (inferior sector). We observed the minimum epiphyseal angle on slices 13 to 2 (superior sector) for both groups.

The alpha angle was higher ($p = 0.001$–0.010) for Group I on slices 8 to 10 (posteroinferior sector), whereas on slice 13 a higher ($p = 0.002$) alpha angle was found for Group II (posterosuperior sector) (Table 5). A bimodal distribution with maximum values for both groups was found on slices 2 to 4 (anterosuperior) and 8 to 9 (posteroinferior sector), respectively. In every single MRI slice the alpha angle was less than or equal to the epiphyseal angle.

Head sphericity and epiphyseal height correlated ($r = 0.536$; $p < 0.001$).

Discussion

Structural deformities of the femoral head occurring during skeletal development (eg, Legg-Calvé-Perthes disease) are associated with individual shapes of the acetabulum but it is not clear whether differences in acetabular shape are associated with differences in proximal femoral shape. We therefore questioned if dysplastic hips have (1) a more aspherical femoral head, (2) a decreased epiphyseal height, (3) a less-pronounced extension of the epiphysis towards the femoral neck, (4) a decreased femoral head neck offset and (5) if a correlation between the femoral head sphericity and the height of the epiphysis can be found.

The main technical limitation of our study is the determination of the femoral head center with the best-fitting

Table 2. Measurement of femoral head morphology and the 3-D extension of the epiphysis*

Parameter	Definition
Head sphericity	Ratio of the minor axis to the major axis of the circle or ellipse drawn to best fit the femoral articular surface
Epiphyseal index [41]	Ratio of the epiphyseal height to width
Epiphyseal angle	Angle formed by the neck axis and a line passing through the center of the head and the point where the epiphysis meets the articular surface
Alpha angle [24]	Angle formed by the neck axis and a line passing through the center of the femoral head and the point where the articular surface exceeds the best-fitting circle

*See Fig. 2 for illustration.

Table 3. Results of reliability

Parameters	ICC Intraobserver 1*	ICC Intraobserver 2*	Interobserver ICC*
Head sphericity	0.82 (0.59–0.92)	0.81 (0.59–0.92)	0.78 (0.63–0.90)
Epiphyseal index	0.85 (0.66–0.94)	0.94 (0.86–0.98)	0.90 (0.81–0.95)
Epiphyseal angle	0.94 (0.85–0.98)	0.96 (0.90–0.98)	0.93 (0.86–0.97)
Alpha angle	0.86 (0.68–0.94)	0.79 (0.55–0.91)	0.81 (0.68–0.91)

ICC = intraclass correlation coefficient; *mean (95% confidence interval).

circle template method according to Mose [21]. If a nonspherical head was present (as was frequently in Group I), the femoral head center was assumed to be the center of the ellipse. A second limitation involves the validity of our results for hips with high-grade dysplasia. We had no hips with a Crowe classification [3] of II or more in our dysplastic group, although we did not specifically exclude them. All dysplastic hips had a congruent joint space without femoral head subluxation. This might be because in severe cases of DDH we obtained no MRI because the indication for surgery was based only on conventional radiography. In addition, the majority of dysplastic hips with subluxation of the joint had been treated surgically earlier. We excluded patients with previous surgery since either acetabular or femoral operations might cause remodeling of the joint [4, 8]. Thus, we cannot draw any inferences on the influence of severe DDH on femoral shape. Finally, we cannot definitely address the issue of causality; whether the femoral head morphology is a result of the acetabular shape or vice versa. However, because we excluded hips with a known history of femoral head pathology or previous surgery, we assume the observed femoral differences in these study groups are mainly due the individual acetabular morphology. Nonetheless, the question of causality could be addressed only in longitudinal studies involving a followup of the growing hip over decades where an initially normal femoral head could be confirmed at an early age.

Various authors state the growth of the hip strongly depends on the interaction between the acetabulum and the femur. Most of these studies suggest a primary abnormality of the femur with subsequent alterations of the acetabulum (eg, in Legg-Calvé-Perthes disease) [4, 6, 9, 10, 12, 18, 19, 32], proximal femoral focal deficiency [5], or slipped capital femoral epiphysis [14]. We are aware of only two reports [8, 26] suggesting variations of acetabular morphology influencing femoral growth. Grzegorzewski et al. [8] reported better long-term remodeling of the femoral head in Perthes hips when a sufficient lateral acetabular coverage was observed initially or when the coverage was improved surgically by pelvic osteotomy or shelf acetabuloplasty. Rejholec and Stryhal [26] described the influence of the acetabular coverage on the development of the proximal femur during the treatment of congenital dysplasia of the hip with varus or Chiari osteotomy.

Several studies describe femoral head morphology in DDH. The majority of the descriptions based on conventional radiography similarly found an elliptical femoral head shape [11, 23, 25, 32, 42]. Siffert [32] even described a "cocked hat deformity." These reports have in common that they only include a 2-D model of the hip in the frontal plane based on plain AP pelvic radiographs. However, the simplification of the complex interaction between the acetabular and femoral shape to a 2-D model might be insufficient. Three-dimensional measurements described in the literature based on CT scans mainly focus on the special morphology of the dysplastic shaft of the proximal femur and its implications for total hip arthroplasty [1, 2, 23, 28, 33]. Previous studies of the epiphysis of the longitudinal growth plate of the femur [32] cannot be

Table 4. Results of head sphericity and epiphyseal index

Parameter	Group	MRI section						
		1/8	2/9	3/10	4/11	5/12	6/13	7/14
Head sphericity*	I	0.83 ± 0.06 (0.70–0.96)	0.80 ± 0.07 (0.65–0.93)	0.81 ± 0.07 (0.64–1.00)	0.83 ± 0.08 (0.65–1.02)	0.87 ± 0.06 (0.73–1.00)	0.87 ± 0.06 (0.72–1.00)	0.82 ± 0.06 (0.71–1.00)
	II	0.99 ± 0.06 (0.88–1.12)	0.97 ± 0.07 (0.78–1.12)	0.98 ± 0.06 (0.86–1.10)	0.99 ± 0.06 (0.86–1.13)	1.00 ± 0.06 (0.86–1.25)	0.99 ± 0.07 (0.88–1.18)	0.97 ± 0.07 (0.84–1.20)
	p Value	< 0.001	< 0.001	< 0.001	< 0.001	< 0.001	< 0.001	< 0.001
Epiphyseal index*	I	0.33 ± 0.05 (0.25–0.46)	0.33 ± 0.05 (0.21–0.43)	0.33 ± 0.06 (0.23–0.50)	0.32 ± 0.05 (0.23–0.41)	0.32 ± 0.05 (0.19–0.45)	0.33 ± 0.06 (0.21–0.50)	0.35 ± 0.05 (0.22–0.48)
	II	0.43 ± 0.04 (0.33–0.57)	0.41 ± 0.05 (0.30–0.55)	0.41 ± 0.05 (0.33–0.51)	0.42 ± 0.06 (0.32–0.62)	0.43 ± 0.05 (0.33–0.54)	0.43 ± 0.05 (0.31–0.55)	0.43 ± 0.04 (0.33–0.54)
	p Value	< 0.001	< 0.001	< 0.001	< 0.001	< 0.001	< 0.001	< 0.001

* Mean ± standard deviation (range).

Table 5. Results of alpha angle and epiphyseal angle

Parameter	Group	MRI section						
		Anterosuperior				Anteroinferior		
		1	2	3	4	5	6	7
Epiphyseal angle*	I	68 ± 9.4 (51–89)	67 ± 12.0 (46–112)	70 ± 11.3 (53–111)	78 ± 8.2 (56–94)	87 ± 8.7 (66–106)	93 ± 8.7 (74–113)	95 ± 8.0 (77–114)
	II	61 ± 7.1 (44–78)	59 ± 7.0 (40–74)	61 ± 6.6 (46–76)	68 ± 7.7 (52–87)	78 ± 8.3 (62–104)	87 ± 7.6 (70–106)	90 ± 10.2 (69–123)
	p Value	< 0.001	< 0.001	< 0.001	< 0.001	< 0.001	< 0.001	0.006
Alpha angle*	I	39 ± 4.8 (26–52)	41 ± 5.9 (31–60)	41 ± 6.0 (32–57)	41 ± 9.8 (26–78)	36 ± 8.1 (24–72)	37 ± 6.7 (25–56)	39 ± 5.3 (31–51)
	II	38 ± 4.8 (25–48)	40 ± 4.9 (30–51)	41 ± 8.1 (22–59)	39 ± 8.6 (24–63)	36 ± 8.2 (21–54)	37 ± 10.4 (23–89)	36 ± 6.2 (23–49)
	p Value	NS	NS	NS	NS	NS	NS	NS

Parameter	Group	MRI section						
		Posteroinferior				Posterosuperior		
		8	9	10	11	12	13	14
Epiphyseal angle*	I	98 ± 9.9 (63–118)	98 ± 11.8 58–120)	95 ± 11.0 (66–118)	82 ± 9.0 (65–107)	72 ± 10.3 (55–99)	64 ± 8.8 (48–84)	65 ± 7.6 (50–84)
	II	95 ± 10.5 (71–120)	94 ± 10.7 (68–115)	86 ± 13.1 (61–118)	71 ± 10.6 (46–103)	64 ± 7.3 (51–68)	60 ± 8.0 (44–80)	60 ± 7.1 (45–80)
	p Value	NS	NS	0.001	< 0.001	< 0.001	NS	0.003
Alpha angle*	I	41 ± 4.9 (30–58)	41 ± 4.9 (31–55)	39 ± 4.6 (24–49)	33 ± 4.4 (23–45)	31 ± 4.1 (22–43)	31 ± 4.0 (19–39)	34 ± 4.2 (27–45)
	II	38 ± 4.3 (27–48)	38 ± 4.7 (24–45)	35 ± 5.1 (19–43)	31 ± 5.9 (22–45)	32 ± 6.8 (19–51)	34 ± 6.8 (19–54)	36 ± 4.8 (23–48)
	p Value	0.01	0.001	< 0.001	NS	NS	0.002	NS

* Mean ± standard deviation (range); NS = not significant.

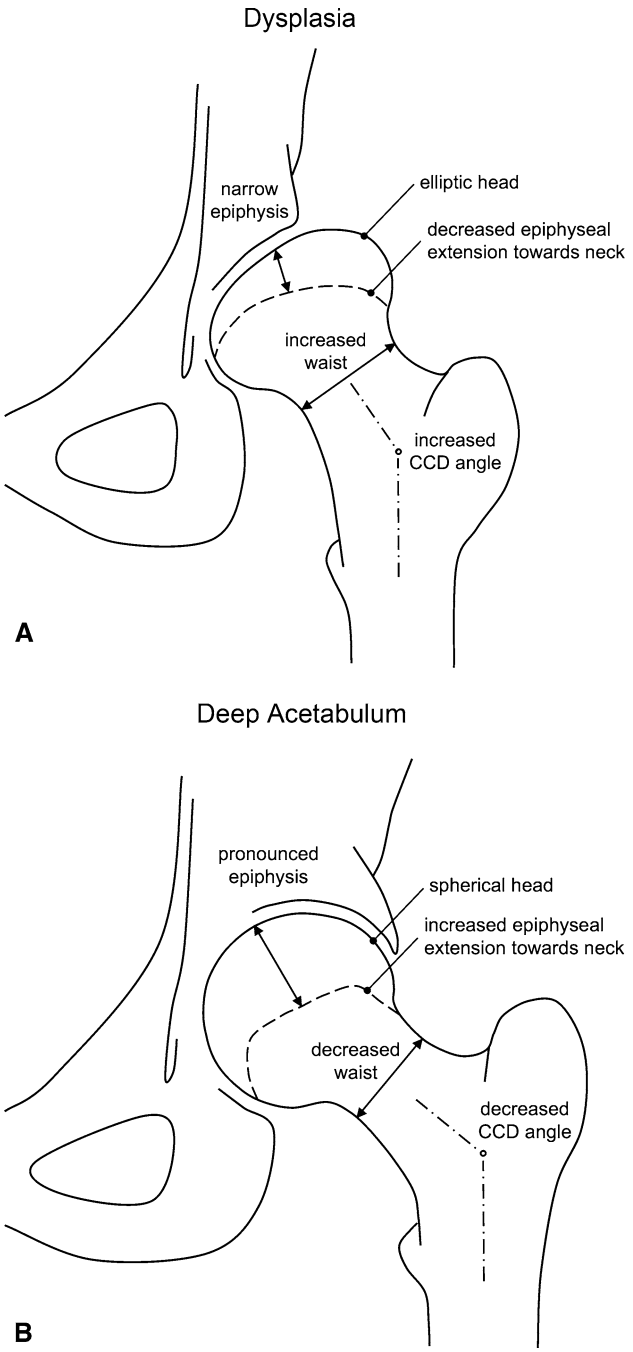

Fig. 5A–B The schematic results of the proximal femoral morphology for (**A**) the dysplasia group (Group I) and (**B**) the deep acetabulum group (Group II) are shown.

compared to our results due to several reasons. They include a wide variation of investigated parameters, the inclusion of femoral-based hip pathologies (eg, Legg-Calvé-Perthes disease [13, 20, 30], cam-type femoroacetabular impingement [31]), and the lack of radial MRI sequences [15, 40]. In addition, none of them investigated the femoral head morphology depending on the acetabular coverage. One reason might be that the problem of "overcoverage" gained interest in the orthopaedic community only in the past few years.

Our observations have clinical implications. When an acetabular reorientation procedure is performed in hips with DDH, the original acetabulum is rotated around an egg-shaped femoral head. This could aggravate the preexisting joint incongruence and lead to early failure. In addition, an elliptical head also gives rise to the speculation of a corresponding nonspherical dysplastic acetabulum. Modern 3-D methods for joint motion and surgical simulation might be used in the future to predict intraarticular dynamic conflicts and incongruity in these cases.

Hips with different acetabular coverage have distinct proximal femoral shapes. A dysplastic hip tends to have an elliptical head, decreased epiphyseal height, decreased epiphyseal extension towards the femoral neck, a valgus neck, and decreased femoral head-neck offset posteroinferiorly. In contrast, overcoverage of the femoral head is associated with a spherical head, increased epiphyseal height, increased epiphyseal extension, a varus femoral neck, and a decreased femoral head-neck offset (Fig. 5A-B). Growth of the femoral head and the acetabulum appears to maintain a mutually dependent relationship in the formation of a congruent hip [32]. The acetabulum seems to require a spherical femoral head as a template for spherical growth [16]. Conversely, the development of a spherical femoral head seems to require a critical minimal amount of acetabular coverage. The abundant coverage as in a deep acetabulum seems to promote spherical growth of the head with a symmetric shape of the epiphysis. However, deficient coverage as occurs in DDH may promote an elliptic head shape with an asymmetric epiphyseal growth. The resulting nonspherical shape of the femoral head and acetabulum can potentially induce a painful femoroacetabular impingement or influence the result of reorientation procedure. As a clinically relevant fact, the resulting nonspherical head in dysplastic hips can lead to joint incongruity after an acetabular reorientation procedure.

References

1. Anda S, Terjesen T, Kvistad KA, Svenningsen S. Acetabular angles and femoral anteversion in dysplastic hips in adults: CT investigation. *J Comput Assist Tomogr*. 1991;15:115–120.
2. Argenson JN, Ryembault E, Flecher X, Brassart N, Parratte S, Aubaniac JM. Three-dimensional anatomy of the hip in osteoarthritis after developmental dysplasia. *J Bone Joint Surg Br*. 2005;87:1192–1196.
3. Crowe JF, Mani VJ, Ranawat CS. Total hip replacement in congenital dislocation and dysplasia of the hip. *J Bone Joint Surg Am*. 1979;61:15–23.
4. Domzalski ME, Glutting J, Bowen JR, Littleton AG. Lateral acetabular growth stimulation following a labral support

procedure in Legg-Calve-Perthes disease. *J Bone Joint Surg Am*. 2006;88:1458–1466.
5. Dora C, Bühler M, Stover MD, Mahomed MN, Ganz R. Morphologic characteristics of acetabular dysplasia in proximal femoral focal deficiency. *J Pediatr Orthop B*. 2004;13:81–87.
6. Ezoe M, Naito M, Inoue T. The prevalence of acetabular retroversion among various disorders of the hip. *J Bone Joint Surg Am*. 2006;88:372–379.
7. Ganz R, Parvizi J, Beck M, Leunig M, Notzli H, Siebenrock KA. Femoroacetabular impingement: a cause for osteoarthritis of the hip. *Clin Orthop Relat Res*. 2003:112–120.
8. Grzegorzewski A, Synder M, Kozlowski P, Szymczak W, Bowen RJ. The role of the acetabulum in Perthes disease. *J Pediatr Orthop*. 2006;26:316–321.
9. Harrison TJ. The influence of the femoral head on pelvic growth and acetabular form in the rat. *J Anat*. 1961;95:12–24.
10. Hochbergs P, Eckerwall G, Egund N, Jonsson K, Wingstrand H. Femoral head shape in Legg-Calve-Perthes disease. Correlation between conventional radiography, arthrography and MR imaging. *Acta Radiol*. 1994;35:545–548.
11. Ito H, Matsuno T, Minami A. Intertrochanteric varus osteotomy for osteoarthritis in patients with hip dysplasia: 6 to 28 years followup. *Clin Orthop Relat Res*. 2005;433:124–128.
12. Joseph B. Morphological changes in the acetabulum in Perthes' disease. *J Bone Joint Surg Br*. 1989;71:756–763.
13. Kendig RJ, Evans GA. Biologic osteotomy in Perthes disease. *J Pediatr Orthop*. 1986;6:278–284.
14. Kitadai HK, Milani C, Nery CA, Filho JL. Wiberg's center-edge angle in patients with slipped capital femoral epiphysis. *J Pediatr Orthop*. 1999;19:97–105.
15. Kumasaka Y, Harada K, Watanabe H, Higashihara T, Kishimoto H, Sakurai K, Kozuka T. Modified epiphyseal index for MRI in Legg-Calve-Perthes disease (LCPD). *Pediatr Radiol*. 1991;21:208–210.
16. Lee MC, Eberson CP. Growth and development of the child's hip. *Orthop Clin North Am*. 2006;37:119–132.
17. Leunig M, Werlen S, Ungersböck A, Ito K, Ganz R. Evaluation of the acetabular labrum by MR arthrography. *J Bone Joint Surg Br*. 1997;79:230–234.
18. Madan S, Fernandes J, Taylor JF. Radiological remodelling of the acetabulum in Perthes' disease. *Acta Orthop Belg*. 2003;69:412–420.
19. Meurer A, Böhm B, Decking J, Heine J. Analysis of acetabular changes in Morbus Perthes disease with radiomorphometry [in German]. *Z Orthop Ihre Grenzgeb*. 2005;143:100–105.
20. Moberg A, Hansson G, Kaniklides C. Results after femoral and innominate osteotomy in Legg-Calve-Perthes disease. *Clin Orthop Relat Res*. 1997;334:257–264.
21. Mose K. Methods of measuring in Legg-Calve-Perthes disease with special regard to the prognosis. *Clin Orthop Relat Res*. 1980;150:103–109.
22. Murphy SB, Ganz R, Müller ME. The prognosis in untreated dysplasia of the hip. A study of radiographic factors that predict the outcome. *J Bone Joint Surg Am*. 1995;77:985–989.
23. Noble PC, Kamaric E, Sugano N, Matsubara M, Harada Y, Ohzono K, Paravic V. Three-dimensional shape of the dysplastic femur: implications for THR. *Clin Orthop Relat Res*. 2003;417:27–40.
24. Nötzli HP, Wyss TF, Stoecklin CH, Schmid MR, Treiber K, Hodler J. The contour of the femoral head-neck junction as a predictor for the risk of anterior impingement. *J Bone Joint Surg Br*. 2002;84:556–560.
25. Pauwels F. Effect of mechanical stress on the skeleton. In: Pauwels F, ed. *Biomechanics of the Normal and Diseased Hip*. New York, NY: Springer;1976:3–7.
26. Rejholec M, Stryhal F. Behavior of the proximal femur during the treatment of congenital dysplasia of the hip: a clinical long-term study. *J Pediatr Orthop*. 1991;11:506–513.
27. Risser JC. The Iliac apophysis; an invaluable sign in the management of scoliosis. *Clin Orthop Relat Res*. 1958;11:111–119.
28. Robertson DD, Essinger JR, Imura S, Kuroki Y, Sakamaki T, Shimizu T, Tanaka S. Femoral deformity in adults with developmental hip dysplasia. *Clin Orthop Relat Res*. 1996;327:196–206.
29. Rosset A, Spadola L, Ratib O. Osiri X: an open-source software for navigating in multidimensional DICOM images. *J Digit Imaging*. 2004;17:205–216.
30. Segev E, Ezra E, Wientroub S, Yaniv M. Treatment of severe late onset Perthes' disease with soft tissue release and articulated hip distraction: early results. *J Pediatr Orthop B*. 2004;13:158–165.
31. Siebenrock KA, Wahab KH, Werlen S, Kalhor M, Leunig M, Ganz R. Abnormal extension of the femoral head epiphysis as a cause of cam impingement. *Clin Orthop Relat Res*. 2004;418:54–60.
32. Siffert RS. Patterns of deformity of the developing hip. *Clin Orthop Relat Res*. 1981;160:14–29.
33. Sugano N, Noble PC, Kamaric E, Salama JK, Ochi T, Tullos HS. The morphology of the femur in developmental dysplasia of the hip. *J Bone Joint Surg Br*. 1998;80:711–719.
34. Tannast M, Mistry S, Steppacher S, Zheng G, Langlotz F, Siebenrock KA. Computer-assisted correction of radiographic parameters on pelvic xrays with Hip^{2}Norm: reliable and validated. In: Langlotz F, Davies BL, Grützner PA, eds. *Computer Assisted Orthopaedic Surgery*. Berlin, Germany: ProBusiness; 2007:88–91.
35. Tannast M, Murphy SB, Langlotz F, Anderson SE, Siebenrock KA. Estimation of pelvic tilt on anteroposterior X-rays–a comparison of six parameters. *Skeletal Radiol*. 2006;35:149–155.
36. Tannast M, Siebenrock KA, Anderson SE. Femoroacetabular impingement: radiographic diagnosis–what the radiologist should know. *AJR Am J Roentgenol*. 2007;188:1540–1552.
37. Tannast M, Zheng G, Anderegg C, Burckhardt K, Langlotz F, Ganz R, Siebenrock KA. Tilt and rotation correction of acetabular version on pelvic radiographs. *Clin Orthop Relat Res*. 2005;438:182–190.
38. Tönnis D. General radiography of the hip joint. In: Tönnis D, ed. *Congenital Dysplasia and Dislocation of the Hip*. New York, NY: Springer; 1987:100–142.
39. Tönnis D, Heinecke A. Acetabular and femoral anteversion: relationship with osteoarthritis of the hip. *J Bone Joint Surg Am*. 1999;81:1747–1770.
40. Tsuchida Y, Kim WC, Takahashi KA, Horii M, Mikami Y, Fujioka M, Kusakabe T, Chang K, Hosokawa M, Kubo T. Usefulness of epiphyseal quotient measurement on magnetic resonance images for outcome prediction in patients with early-stage Legg-Calve-Perthes disease. *J Pediatr Orthop B*. 2005;14:16–23.
41. Wiberg G. The anatomy and roentgenographic appearance of a normal hip joint. *Acta Chir Scand*. 1939;83:7–38.
42. Yanagimoto S, Hotta H, Izumida R, Sakamaki T. Long-term results of Chiari pelvic osteotomy in patients with developmental dysplasia of the hip: indications for Chiari pelvic osteotomy according to disease stage and femoral head shape. *J Orthop Sci*. 2005;10:557–563.
43. Zheng G, Tannast M, Anderegg C, Siebenrock KA, Langlotz F. Hip^{2}Norm: An object-oriented cross-platform program for 3D analysis of hip joint morphology using 2D pelvic radiographs. *Comput Methods Programs Biomed*. 2007;87:36–45.